Closures for multicomponent reacting flows based on dispersion analysis

Omkar B. Shende* and Ali Mani†
Department of Mechanical Engineering, Stanford University, Stanford, California 94035, USA

(Received 24 November 2021; accepted 1 August 2022; published 12 September 2022)

This work presents algebraic closure models associated with advective transport and nonlinear reactions in a Reynolds-averaged Navier-Stokes context for a system of species subject to binary reactions and transport by advection and diffusion. Expanding upon analysis originally developed for non-reactive transport in the context of Taylor dispersion of scalars, this work extends the modified gradient diffusion model explicated by Peters [N. Peters, Turbulent Combustion, Cambridge Monographs on Mechanics (Cambridge University Press, Cambridge, 2000)] and based on work by Corrsin [S. Corrsin, The reactant concentration spectrum in turbulent mixing with a first-order reaction, J. Fluid Mech. **11**, 407 (1961)] beyond single-component transport phenomena and involving nonlinear reactions. The presented model forms, from this weakly nonlinear extension of the original dispersion theory, lead to an analytic expression for the eddy diffusivity matrix that explicitly captures the influence of the reaction kinetics on the closure operators. Furthermore, we demonstrate that the derived model form directly translates between flow topologies through *a priori* and *a posteriori* testing of a binary species system subject to homogeneous isotropic turbulence. Using two- and three-dimensional direct numerical simulations involving laminar and turbulent flows, it is shown that this framework improves prediction of mean quantities compared to previous results. Lastly, the presented model form, collapses to the earlier gradient diffusion and its modified version derived by Corrsin in the limits of nonreactive species and linear reactions, respectively.

DOI: 10.1103/PhysRevFluids.7.093201

I. INTRODUCTION

Building reduced-order models for turbulent reacting flows is theoretically and computationally challenging as the underlying chemical and transport processes are individually complex and a thorough understanding of the coupled effects of these phenomena remains elusive. However, deeper insight into the mechanisms by which turbulent transport and reaction dynamics influence each other is essential for the future design of efficient systems. In particular, finding models that capture the influence of microscale fluctuations on macroscale quantities is a key problem in computational predictive science and has applications involving atmospheric [1] and marine pollution, combustion [2], electrolyte solutions in electrochemical applications [3], and related fields.

When considering a system of reactive scalars, the simplest possible multicomponent setup would involve a single-step chemistry with two reacting species. The reaction rate is physically temperature dependent and the heat release from the reaction and the changing concentration of scalars both couple the scalar fields to the velocity field. Direct simulations of these fields are prohibitively expensive due to the excessive temporal and spatial resolution requirements. As a rem-

*oshende@stanford.edu
†alimani@stanford.edu

edy, computational models often seek reduced-order representations in terms of ensemble-averaged fields [1], homogenized fields [4], or spatially filtered fields. [5] In each of these methods, there exist microscale features whose effects are not explicitly simulated but which affect the macroscale quantities and must be accounted for via closure models.

To account for microscale effects on transport terms, a gradient transport assumption is often invoked, but models using this assumption often contain parameters that are agnostic to reaction [2,5]. As these system often involve reaction nonlinearity, reaction terms themselves involve closure problems which should be additionally captured via closure models that must also be informed by both chemical kinetics and turbulence.

The goal of this study is to demonstrate how even a highly-simplified reaction coupling leads to a model form for transport closures that explicitly incorporates chemical effects. Said more explicitly, we would like to demonstrate that, in the presence of even the simplest of chemistry mechanisms, the effective diffusivity intended for capturing transport closure for one scalar should depend on other scalar fields and their gradients. A model so developed might not be immediately suitable for application to a realistic setup with energetic reactions, such as highly turbulent deflagrations, but offers qualitative insights into the requirements for expected model forms that would apply to even those cases.

With this in mind, let us consider the most fundamental chemical system with constant reaction coefficients and no thermal expansion effects as a simplification to other flows in which the reaction coefficient is variable (i.e., temperature dependent) and dilatation effects are not negligible. In considering the evolution of the concentration of passive scalars in such an incompressible flow, a one-way coupling between the fluid momentum and the scalars is typically assumed in writing the transport equations. In particular, if considering the concentrations of two scalars involved in a binary reaction system, the concentrations being denoted C_1 and C_2, in an imposed solenoidal velocity field, U, the governing equations can be formulated as

$$\frac{\partial C_i}{\partial t} + \nabla \cdot (UC_i) = D_m \nabla^2 C_i - AC_i C_{j\neq i}, \tag{1}$$

where A is a reaction coefficient and D_m is a scalar diffusivity which is assumed to be the same for both indexed scalars in this work. This equation is valid in the dilute limit, where the heat release from the reaction is so small as to affect neither the density nor the reaction kinetics [6].

While this form of the equation incorporates all effects in the system, in practice, the Reynolds-averaged version of Eq. (1), written as

$$\frac{\partial \overline{C_i}}{\partial t} + \nabla \cdot (\overline{U}\,\overline{C}_i) + \nabla \cdot (\overline{U'C'_i}) = D_m \nabla^2 \overline{C_i} - A\overline{C}_i \overline{C}_{j\neq i} - A\overline{C'_i C'_{j\neq i}}, \tag{2}$$

has more utility due to its lower computational cost to solve when compared to the full degree-of-freedom system. In Eq. (2), the primed terms denote fluctuations about the mean quantities, which are denoted by over-bars. In general, for a stochastic system, this averaging is done over multiple ensembles of flow realizations, and the corresponding set of partial differential equations for the velocity field are the Reynolds-averaged Navier-Stokes (RANS) equations. Finding models for the two types of unclosed terms in Equation 2, $\overline{U'C'_i}$ and $\overline{C'_i C'_{j\neq i}}$, allows for the entire problem to be solved. In this work, such a model will be derived using a weakly-nonlinear extension of dispersion analysis.

A. Taylor dispersion

For nonreacting scalar contaminants, many models exist for tracking the dispersion of passive scalars. The most common analytic model invoked for the unclosed transport term in the nonreactive equations, which is also used for some reactive cases, follows the generalized gradient diffusion

hypothesis, for which the unresolved flux of a single passive scalar is of the form

$$\overline{u_i' C_1'} = -D_{\text{eff}} \frac{\partial \overline{C_1}}{\partial x_i}, \tag{3}$$

where D_{eff} is a generic effective eddy diffusivity that aggregates turbulent transport effects. When there is strong scale separation between the mean fields and the underlying fluctuating velocity fields, this local model is exact, with the caveat that D_{eff} may be a nonisotropic tensor when the underlying fluctuating flow is not statistically isotropic. [7,8]

In the framework of this model form, there is a rich body of literature on analytic models that find this effective diffusivity in canonical flows. In this study we denote the effective diffusivity in the absence of reaction as D^0, and refer to it as the "standard" eddy diffusivity. Correspondingly, we denote $D_{\text{eff}} = D^0$ as referring to the standard gradient diffusion model, which is agnostic to the reactivity of scalars.

There are many ways to measure this defining parameter. In particular, for the case of parallel flow in a pipe, [9] shows that a passive scalar experiences enhanced diffusive transport in the longitudinal direction. We can define an axial Péclet number as $Pe \sim uL/D_m$ such that, at high values of the Péclet number, D^0 dominates the standard molecular diffusivity, D_m. In parallel flows, it is generally shown that this quantity scales as

$$\frac{D_0}{D_m} \sim \frac{u^2 L^2}{D_m^2}, \tag{4}$$

where u is the characteristic convective speed, and L is some characteristic spanwise length scale for the flow. This idea can be expanded to applications outside of pipe flow, and other studies have expanded the range of problems and fields to ones that Taylor's original analysis does not address. [10–13]

B. Other scalar transport models

Thus far, we have only looked at nonreactive models. However, many tracers of interest are not passive; to reach a multicomponent framework, the first step is the simplest possible reaction involving two species, where the concentration of the second species is orders of magnitude larger than the first everywhere in the domain. In some applications, this allows an assumption that the second species is maintained in the domain at a constant concentration and unaffected by the reaction dynamics, leading to a first-order linear reaction term for the first species. In the presence of such a first-order linear reaction, [2] used work by Ref. [14] to propose a model that incorporates the chemistry effects for the unclosed scalar flux term. It can be written as

$$\overline{u_i' C_1'} = -\frac{D^0}{1 + A\overline{C_2}\tau_{\text{mix}}} \frac{\partial \overline{C_1}}{\partial x_i}. \tag{5}$$

In this model, τ_{mix} is a characteristic time scale for mixing by the flow. In the denominator, one can form a Damköhler number, relating the timescale of the reaction to the turbulence time scale, and can therefore write the flux as the gradient times an effective diffusivity that scales as

$$D_{\text{eff}} \sim \frac{D_0}{1 + Da}, \tag{6}$$

where D^0 is the aforementioned "standard" turbulent diffusivity. When the reaction rate is sufficiently slow or when examining the nonreacting limit where Da vanishes, this recovers the gradient diffusion model exactly. While D^0 still needs to be determined from other means, the advantage of Equation 6 is that it analytically captures the impact of reaction on D_{eff}.

Equation 6 contributes critical understanding by explicitly revealing the dependence of effective diffusivity (or eddy diffusivity) on the reaction kinetics and, specifically, the reaction coefficient. Although transport and kinetics are controlled by independent terms at the microscopic continuum

level, when behavior at a macroscopic level, governed by ensemble-averaged equations, is sought, kinetics influence transport.

In this study, we develop a model in the Reynolds-averaged context that can provide algebraic closures to the scalar evolution equations for a binary reactant setup. We do this using the spirit of Taylor's dispersion analysis. By considering the case of a parallel flow as an analytical prototype, we extend Taylor's analysis to discover model forms for dispersion of scalars undergoing binary reactions. Given the nonlinearity of this system, the closure operators are expected to be dependent on the transported quantity itself. We derive these dependencies through a weakly nonlinear extension of Taylor's original analysis. We then hypothesize that reactive mixing by turbulent flows should involve model forms with similar nonlinearities, but with different model coefficients. This is analogous to the situation of nonreactive scalars, where mixing by both classes of flows can be reasonably captured by gradient diffusion models. However, the diffusivity coefficients differ based on the underlying flow topology, with D^0/D_M scaling as Pe^2 in parallel flows and as Pe^1 in turbulent flows.

Our weakly nonlinear model offers improvements to perturbation expansions based on directly linearizing the equations performed by works like Ref. [4]. It also recovers the scaling relationship between diffusivity and Damköhler number derived in Refs. [15] and [16], although those works use nonlinear first-order reactions. It also indicates that the effective eddy diffusivity is linked to reaction, as has been shown in experiments. [17] This relationship shows that the impacts of reaction chemistry and turbulent mixing are fundamentally linked and even with simple flows, we will see complex features arising in the RANS model, such as cross diffusion coefficients with a dependence on reaction rates and local concentrations. As such, we can expect complex cases are unlikely to be simpler than this scenario, and even more complex model forms will need to be discovered.

In what follows, we will first develop a model problem based on laminar flows that can capture the relevant multi-physics at play for a linear reaction setup and work to find a solution for the single-scale and the multi-scale problems. This insight will guide generalization to a binary reaction problem, which we can fully expand to general turbulent flows. The outcome of our analysis is a unifying reduced-order model (ROM) in the RANS context that captures the analytic impact of chemical kinetics on transport and reaction closures while leveraging existing literature on nonreactive scalar transport modeling.

II. MODEL PROBLEM

In order to develop insights into a model form that captures closure terms in a binary mixture, we propose the following illustrative setup that can be treated semianalytically. Consider a flow field that is parallel, steady, and two-dimensional (2D), contained in a domain that is an elongated box. We place periodic boundary conditions on the two opposing elongated sides, as seen in Figure 1. By elongated, we mean that $L_1 \gg L_2$.

In such a two-dimensional domain, we define an averaging operator as

$$\overline{f(x)} = \frac{1}{L_2}\int_0^{L_2} f(x,y)dy, \tag{7}$$

which differs from the ensemble averaged used earlier. In this context, let us use a periodic structure for the flow-field which imposes no mean velocity. Namely, $u(x,y) = \overline{u} + u' = U_0\sin(ky)$ and $v(x,y) = 0$, where $k = 2\pi/L_2$. At $x = -L_1/2$ and $x = L_1/2$, the two domain boundaries, we prescribe Dirichlet conditions for the scalar concentrations.

In addition, we consider a reaction of the form $C_1 + C_2 \rightarrow C_3$, which is considered irreversible and fully activated, but follows a finite rate law of mass action. While simpler than a fully three-dimensional turbulent flow with reacting scalars, this model problem captures the essential competing physics of mixing, transport, and reactions that are present in the more realistic case. However, we can now formulate solutions in this sandbox context and propose closures for each subproblem that each highlight different aspects of the overall ROM.

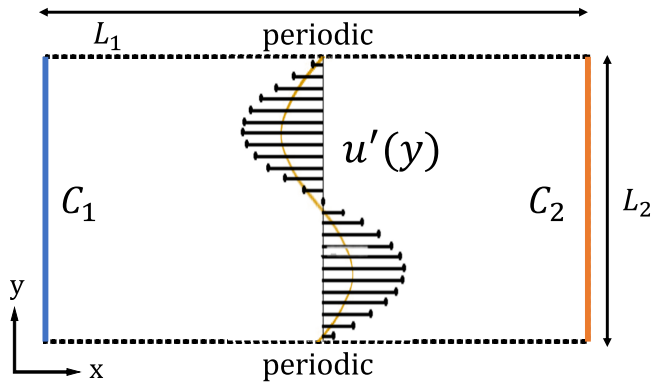

FIG. 1. A schematic of the model problem, illustrating dimensions and boundary conditions. The flow is depicted in black as $u'(y)$, with a representation of a reaction front given at the mid-plane. Axial will refer to the x direction, while spanwise will refer to the y direction

A. Linear reaction, single-scale flow

Let us first examine this problem in the context of a linear reaction. In this setup, the concentration of one of the scalars, C_2, is held constant in the entire domain at unity and does not evolve, while the maximum value of C_1, at the left side of the domain, is held to be at least an order of magnitude less than that of C_2. As C_2 is a constant, we will denote the reaction rate as $A_L = AC_2$, denoting the product of a standard binary species reaction coefficient times the concentration of the constant species. The fluctuations for C_1 are governed by a transport equation as

$$\frac{\partial C_1'}{\partial t} + \frac{\partial (u' C_1')'}{\partial x_1} + u'(y)\frac{\partial \overline{C_1}}{\partial x_1} = D_m \frac{\partial^2 C_1'}{\partial x_i \partial x_i} - A_L C_1', \tag{8}$$

where $C_1 = \overline{C_1} + C_1'$ and so on. This equation can be derived by finding the classical transport equation for C_1 and subtracting from it the evolution equation for $\overline{C_1}$. Note that we have implicitly assumed here that the molecular diffusivity, D_m, is the same for all species, is constant, and is isotropic. In addition, the flow has only a single nonzero component, so all advection terms involve only the axial velocity field.

This equation is similar to the equation governing evolution of fluctuating fields in the work of Ref. [9], with the primary distinction being the reaction term on the right-hand side. While Taylor was not explicitly considering this type of periodic parallel flow in his work, the steps he follows allow us to also simplify this equation to arrive at a more analytically approachable differential equation.

First, we note that we are considering a domain where $L_1 \gg L_2$, from which we can conclude that diffusion in the axial direction, x, can be neglected when compared to diffusion in the spanwise direction y. This can be shown by performing a scaling analysis and seeing the associated term tends to zero as the relevant axial Péclet number tends to infinity. This allows us to neglect axial diffusion in Equation 8.

In addition, when $L_1 \gg L_2$, the time scale of mixing in the axial direction is much larger than the time scale of mixing in the spanwise direction. Therefore, one can decompose the concentration field as $C_1(x, y) = \overline{C_1}(x) + C_1'(x, y)$, allowing for evolution of the mean field in the axial direction but considering the underlying field to be "well mixed" in the spanwise direction. In particular, the presence of fast mixing in the spanwise direction implies that $|C_1'| << |\Delta\overline{C_1}|$, where $|\Delta\overline{C_1}|$ is a characteristic change in the averaged concentration in the axial direction.

This final conclusion allows us to see that the second term on the left-hand side of Equation 8 must be much less significant than the advection of the mean scalar concentration, represented by

the third term on the left-hand side. Therefore, for a leading-order approximation, we can neglect the former, double primed term.

All of these physical assumptions imply that the flow is in an advection-driven limit. The strong mixing in the spanwise direction that such a flow implies also allows us to invoke a quasisteady approximation for the evolution of the fluctuating concentration. In particular, since we are most interested in the long-time response, not the initial transient one, this assumption does not unreasonably limit our analysis.

If the previous simplifications are applied to Equation 8, the dominant remaining terms give us an approximate evolution equation that can be written as

$$u'(y)\frac{\partial \overline{C_1}}{\partial x} = D_m \frac{\partial^2 C_1'}{\partial y^2} - A_L C_1'. \tag{9}$$

This gives us the dispersion of the fluctuating quantity as driven by the flow. A further ansatz we make here is that the form of the fluctuating components follows the velocity, as $C_1(x, y) = \overline{C_1}(x) + f_1(x)\sin(ky)$. That is, the fluctuating field has some magnitude determined purely by axial position. This is motivated by examining solely the leading-order term in the harmonic expansion of the concentration fluctuations in the y direction. Substituting this into the fluctuation equation yields

$$D_m k^2 f_1(x) + A_L f_1(x) = -U_0 \frac{\partial \overline{C_1}}{\partial x}. \tag{10}$$

Solving this equation for our unknown axial concentration magnitude yields

$$f_1(x) = -\frac{U_0}{k^2 D_m + A_L}\frac{\partial \overline{C_1}}{\partial x}. \tag{11}$$

The only unclosed term in Equation 8 is the scalar flux, and it can now be solved as

$$\overline{u'C_1'} = \overline{U_0 f_1(x)\sin^2(ky)} = -D_{\text{eff}}\frac{\partial \overline{C_1}}{\partial x}. \tag{12}$$

Here, D_{eff} is given by

$$D_{\text{eff}} = \frac{D^0}{1 + A_L \tau_{\text{mix}}}, \tag{13}$$

where the standard eddy diffusivity, D^0, is determined from nonreactive Taylor-type analysis. For this flow, it is given by

$$D^0 = \frac{U_0^2}{2D_m k^2}. \tag{14}$$

In addition, τ_{mix} is a characteristic time scale for mixing given by

$$\tau_{\text{mix}} = \frac{1}{D_m k^2} = \frac{D^0}{u_{\text{rms}}^2}, \tag{15}$$

where u_{rms} is the root-mean-squared velocity of the underlying flow, equal to $U_0/\sqrt{2}$ in this derivation.

For this section, we will refer to Equation 5 as the linear reaction model and Equation 13 as a special case of our reduced-order model (ROM) for this first-order reaction context.

Interestingly, for this problem, the ROM is identical to Equation 5, even though it is derived in a laminar context, while the latter was created in the framework of turbulent flows. It again has an effective Damköhler number in the denominator, and shows that effective diffusivity decreases as the reaction rate increases relative to the flow time scale. This lends confidence that the choice of model problem should not hinder the relevance of the conclusions here in application to turbulence.

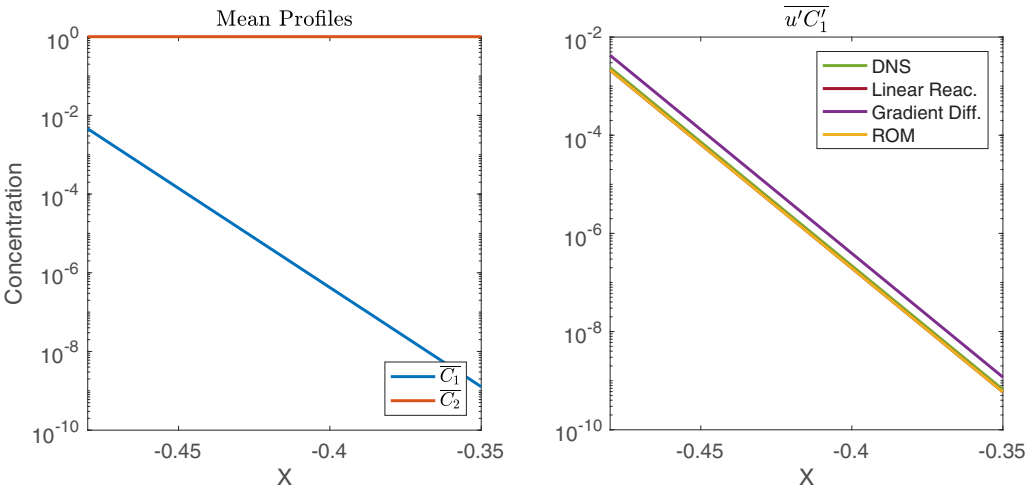

FIG. 2. Predictions of closures for the linear reaction problem subject to a turbulent flow, $X = x/L_1$. The linear reaction model of Equation 5 is identical to the ROM represented by Equation 12, and the former is overlaid by the latter in the plot.

In particular, the model form is an explicit function of A_L, with the other two quantities, D^0 and u_{rms}, defined purely in terms of flow parameters. This means that they can be derived independent of the reaction kinetics, in nonreacting flow, and applied directly to this model for reacting flows.

To test this model, we next examine its predictions against 2D Direct numerical simulation (DNS) data as well as the gradient diffusion model that ignores impact of reactions on the advective closure. For this purpose, we consider a setting with axial $Pe \equiv (U_0 L_2)/(2\pi D_m) = 100$, and $Da \equiv A_L \tau_{\text{mix}} = 1$. For the axial boundary conditions, we used Dirichlet conditions $x = -L_1/2$ and $x = L_1/2$ by, respectively, enforcing C_1 to be equal to 0.1 and 0.

Figure 2 presents quantitatively a comparison between different results. For this specific setting, the mean concentration assumes an exponential profile, as seen in the figure. It can be seen that ROM produces results much closer to the DNS than the gradient diffusion model. The gap between DNS and gradient diffusion model is solely due to over prediction of D_{eff} by the model. For settings at higher Da values, the correction offered by ROM becomes even more crucial as this gap will be even larger. In this setting, there is no unresolved flux of C_2.

B. Linear reaction, multiscale flow

The previous section only considered a velocity field with a single relevant length scale. However, a realistic flow has a spectrum of relevant scales and the model problem setup allows us to consider a straightforward superposition of multiple velocity fields. The total velocity now can be represented by $u(x, y) = \sum U_n \sin(nky)$, where $k = 2\pi/L_2$ and n refers to each scale as corresponding to an integer multiple of the fundamental scale set by k. Following the same procedure as the previous section, the unresolved scalar flux can be expressed as

$$\overline{u'C_1'} = -D_{\text{eff}} \frac{\partial \overline{C_1}}{\partial x}, \tag{16}$$

where D_{eff} is written as

$$D_{\text{eff}} = \sum_{n=1}^{\infty} \frac{U_n^2/2}{n^2 k^2 D_m + A_L}. \tag{17}$$

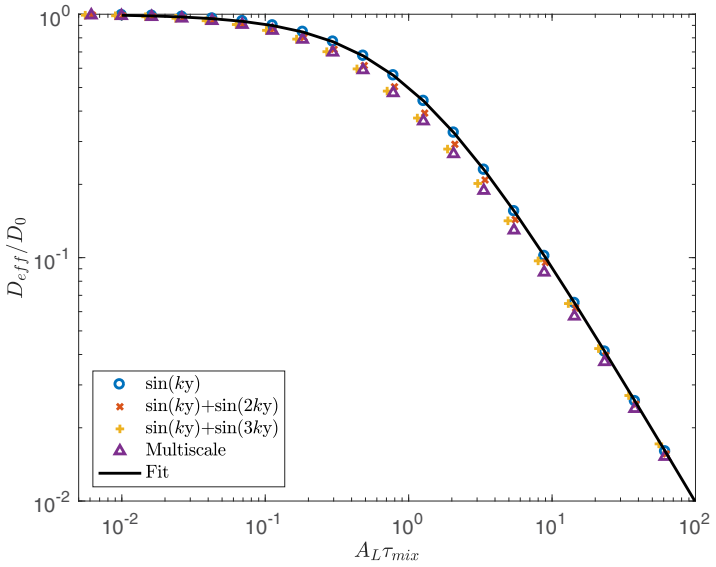

FIG. 3. Effective diffusivity calculated as a function of $Da = A_L\tau_{\text{mix}}$. D_{eff} is calculated using Equation (17) and D^0 is calculated using Equation (19). Each marker refers to a different velocity field specified in the figure legend, with the "multiscale" field given by Equation 21. The solid line represents Equation 18.

In this context, the dependence of D_{eff} on A_L is more complex. Nevertheless, we still seek to express the dependence of D_{eff} on A in terms of a simple expression that involves low order statistics, specifically D^0 and u_{rms}. In order to do so, we first examine the expression above in the asymptotic limits of large and small A_L. In the limit of A_L equaling zero, the above expression results in D_{eff} equal to the D^0 of the multiscale flow field, recovering the nonreactive solution from pure Taylor-type analysis. In the limit of large A_L, however, we obtain that $D_{\text{eff}} = u_{\text{rms}}^2/A_L$.

Interestingly, examining Equation 13 and updating values for D^0 and τ_{mix} satisfies both limits exactly:

$$D_{\text{eff}} = \frac{D^0}{1 + A_L\tau_{\text{mix}}}, \tag{18}$$

where now

$$D^0 = \sum_{n=1}^{\infty} \frac{U_n^2/2}{n^2k^2D_m} \tag{19}$$

and τ_{mix}, the mixing time, is D^0/u_{rms}^2, with

$$u_{\text{rms}}^2 = \sum_{n=1}^{\infty} U_n^2/2. \tag{20}$$

We reiterate that both D^0 and u_{rms}, and therefore τ_{mix}, are fundamental measures of the flow that are independent of the presence of the reaction, and there is no A_L dependence in these quantities.

One can examine this model by comparing the D_{eff} it provides against those from Equation 16, as shown in Fig. 3. Among the various velocity profiles tested, we considered the following velocity profile, denoted as 'multiscale" in Fig. 3, expressed as

$$u'(y) = \sum_{n=1}^{10} n^{-5/6}\sin(nky), \tag{21}$$

to mimic the multiscale effects found in turbulence. The specific power, $-5/6$, is chosen such that the eddy diffusivity at each wave number matches that of Kolmogorov turbulence.

In Fig. 3, the simple model presented in Equation 18 is plotted across values of the reaction rate. These results come from plotting the relevant equations and not from full flow simulations. We see that the model captures the precise behavior of D_{eff} in the limits of small and large A_L across a variety of imposed velocity fields. Additionally, the model still fits the data reasonably in the intermediate regimes where $A_L\tau_{\text{mix}} \sim O(1)$.

C. Binary reaction

Having some confidence with the linear problem, we now turn back to examining Equation 2 in its entirety, and note that the complete problem involves a full binary system, where both C_1 and C_2 are free to evolve.

Before proceeding with derivation of a closure model, let us first test whether we can naively modify Equation 5 to perform reasonably in the case of binary reactions. Specifically, one may interpret that for evolution of each species, C_i, the other species might be assumed "locally constant." This allows interpreting an effective A_L for each species as $A_L = A\overline{C}_{j\neq i}$. With this simple modification, the previous model form can be extended to a multiscale model as

$$\overline{u'C_i'} = -\frac{D}{1 + A\tau\overline{C_j}}\frac{\partial\overline{C_i}}{\partial x}, \tag{22}$$

where A_L is now replaced with the $A\overline{C_2}$ and $A\overline{C_1}$ for mean advective fluxes associated with C_1 and C_2, respectively.

We next examine the performance of this model form by comparing its prediction against direct numerical simulation. In this case we consider a single-scale velocity profile where $u(y) = U_0\sin(ky)$, but where both reactants are now free to vary. We choose axial $\text{Pe} \equiv (U_0L_2)/(2\pi D_m) = 100$ and $Da \equiv A\tau_{\text{mix}}C_{\text{ref}} = 100$, where C_{ref} is concentration imposed by Dirichlet boundary conditions on each scalar. More specifically, the boundary condition on $C_1 = C_{\text{ref}}$ is imposed at $x = -L_1/2$ and $C_2 = C_{\text{ref}}$ is imposed at $x = L_1/2$. The other boundary condition for each scalar is a homogeneous Dirichlet condition.

In Fig. 4, we see that the linear reaction model given by Equation 22 incurs great errors near the middle of the domain, where C_1 and C_2 exist in near-stoichiometric ratios. Surprisingly, the standard gradient diffusion model, which carries no chemistry information, now outperforms this more physics-based model.

Clearly, the linear reaction model is not sufficient to describe this system, so let us return to Equation 2 and examine the full system of equations again. In this framework, the governing equations for the fluctuations control the evolution of the unclosed terms of interest. For C_1, this looks like

$$\frac{\partial C_1'}{\partial t} + \frac{\partial(u'C_1')'}{\partial x_1} + u'(y)\frac{\partial\overline{C_1}}{\partial x_1} = D_m\frac{\partial^2 C_1'}{\partial x_i\partial x_i} \quad - A\overline{C_1}C_2' - A\overline{C_2}C_1' \quad + A(C_1'C_2')'. \tag{23}$$

Again following the work of Ref. [9], we can add one more assumption for the binary system that was not relevant for the linear case, which is that the fluctuations of the product of fluctuating quantities will be negligible when compared to the mean-field quantities.

If those simplifications are applied to Equation 23 for C_1, it can be reformulated as

$$u'(y)\frac{\partial\overline{C_1}}{\partial x} = D_m\frac{\partial^2 C_1'}{\partial y^2} - A\overline{C_1}C_2' - A\overline{C_2}C_1', \tag{24}$$

and an equivalent equation can be derived for C_2.

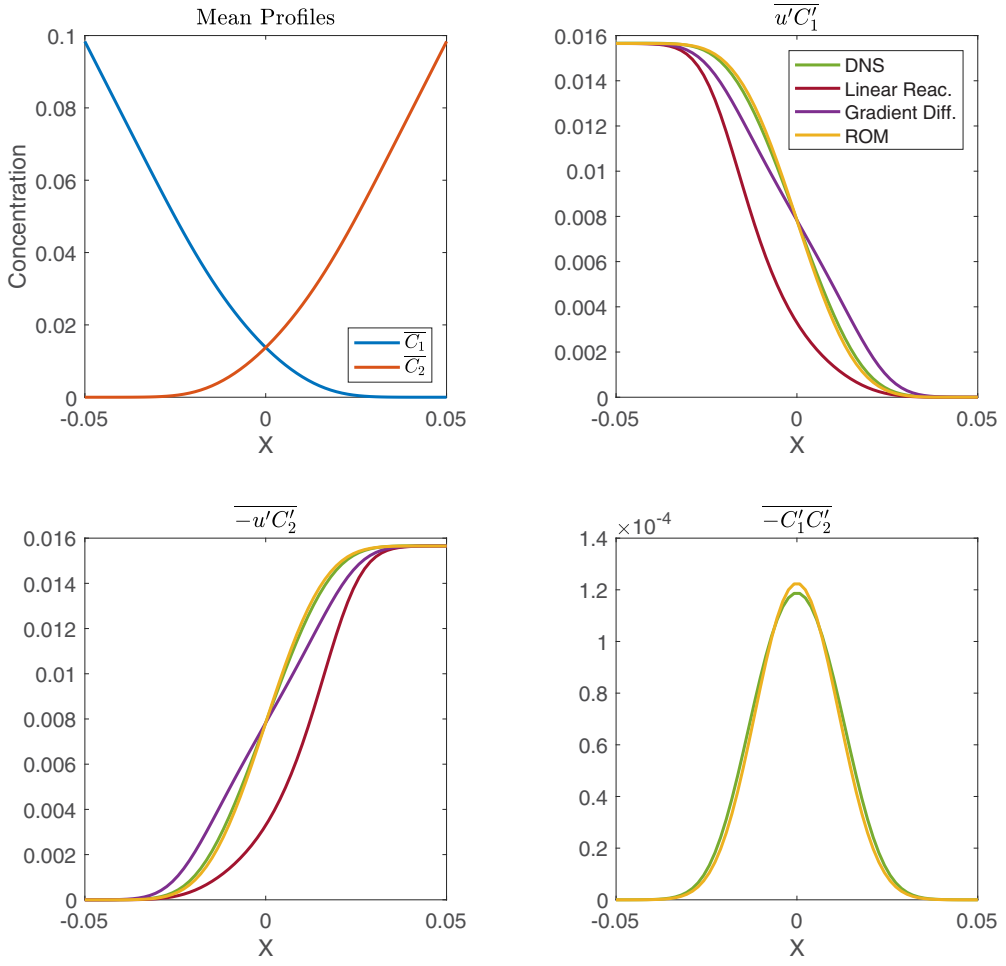

FIG. 4. Predictions of closures for the binary reaction problem subject to a laminar flow, $X = x/L_1$.

We again make the ansatz that $C_i(x, y) = \overline{C_i}(x) + f_i(x)\sin(ky)$, following the velocity. Substituting this into the fluctuation equations yields the following system of two equations:

$$D_m k^2 f_1(x) + A\overline{C_1} f_2(x) + A\overline{C_2} f_1(x) = -U_0 \frac{\partial \overline{C_1}}{\partial x} \tag{25}$$

and

$$D_m k^2 f_2(x) + A\overline{C_2} f_1(x) + A\overline{C_1} f_2(x) = -U_0 \frac{\partial \overline{C_2}}{\partial x}. \tag{26}$$

This is a coupled, but linear, set of equations for f_1 and f_2 that can be solved to find that

$$f_1(x) = \frac{-U_0(k^2 D_m + A\overline{C_1})}{k^2 D_m(k^2 D_m + A\overline{C_1} + A\overline{C_2})} \frac{\partial \overline{C_1}}{\partial x} + \frac{U_0(A\overline{C_1})}{k^2 D_m(k^2 D_m + A\overline{C_1} + A\overline{C_2})} \frac{\partial \overline{C_2}}{\partial x} \tag{27}$$

and

$$f_2(x) = \frac{-U_0(k^2 D_m + A\overline{C_2})}{k^2 D_m(k^2 D_m + A\overline{C_1} + A\overline{C_2})} \frac{\partial \overline{C_2}}{\partial x} + \frac{U_0(A\overline{C_2})}{k^2 D_m(k^2 D_m + A\overline{C_1} + A\overline{C_2})} \frac{\partial \overline{C_1}}{\partial x}. \tag{28}$$

We can also write these terms, the result of using a weakly nonlinear extension of dispersion analysis, as the superposition of two gradients multiplied by a prefactor representing an effective diffusivity. The equations for the scalar flux now look like

$$\begin{bmatrix} \overline{u'C_1'} \\ \overline{u'C_2'} \end{bmatrix} = -\begin{bmatrix} D_{11} & D_{12} \\ D_{21} & D_{22} \end{bmatrix} \frac{\partial}{\partial x} \begin{bmatrix} \overline{C_1} \\ \overline{C_2} \end{bmatrix}, \tag{29}$$

where D_{kl} represents a diffusivity associated with the flux of the kth species due to gradient in the lth species. The square matrix formed by these coefficients also has positive eigenvalues so long as the mean scalar fields maintain their positivity. The coefficients are written as

$$\begin{aligned} D_{11} &= \frac{D^0(1 + A\overline{C_1}\tau_{\text{mix}})}{1 + A\tau_{\text{mix}}\overline{C_1} + A\tau_{\text{mix}}\overline{C_2}}, \quad D_{12} = -\frac{D^0 A\tau_{\text{mix}}\overline{C_1}}{1 + A\tau_{\text{mix}}\overline{C_1} + A\tau_{\text{mix}}\overline{C_2}}, \\ D_{21} &= -\frac{D^0 A\tau_{\text{mix}}\overline{C_2}}{1 + A\tau_{\text{mix}}\overline{C_1} + A\tau_{\text{mix}}\overline{C_2}}, \quad D_{22} = \frac{D^0(1 + A\overline{C_2}\tau_{\text{mix}})}{1 + A\tau_{\text{mix}}\overline{C_1} + A\tau_{\text{mix}}\overline{C_2}}, \end{aligned} \tag{30}$$

using the notation from Sec. II A.

Perhaps most novel, however, is that determining the actual local form of the fluctuations means it is now possible to close not only the scalar transport term, but also the unclosed reaction terms in the standard RANS equations. This closure equation looks like

$$\overline{AC_1'C_2'} = \frac{A}{u_{\text{rms}}^2}\left(D_{11}\frac{\partial\overline{C_1}}{\partial x} + D_{12}\frac{\partial\overline{C_2}}{\partial x}\right)\left(D_{21}\frac{\partial\overline{C_1}}{\partial x} + D_{22}\frac{\partial\overline{C_2}}{\partial x}\right). \tag{31}$$

This provides our ROM in its most complete form. It solves a reduced-degree-of-freedom system resulting from the RANS equations. The three algebraic components describe an entire model form, and require only prescriptions of parameters of the underlying flow, specifically D^0 and u_{rms}. It is important to note that this model, under the appropriate limits, captures the gradient diffusion model and the linear reaction as its special cases. The gradient diffusion model is realized in the limit of $A \to 0$. The linear reaction model, for finite A_L, can be realized in the limit of $\overline{C_2} \to \infty$ and $A \to 0$.

Comparing this model against the DNS data presented in Fig. 4, we see that the new model recovers from the errors of the Linear Reaction model, and outperforms the Gradient Diffusion model.

We have neglected multiple terms in this derivation of the presented ROM. In Supplemental Material [18], we provide a higher-order correction to the ROM that adds in nonlinear effects and demonstrate this further reduces the error in the context of this laminar problem.

III. APPLICATION TO TURBULENT FLOWS

Now that we have built up the full ROM, we can turn to realistic turbulent flows. A great strength of the approach used in the previous section is that we can borrow the model form from the laminar analysis directly and use it in an analogous domain of homogeneous, isotropic turbulence. For this flow configuration, as a recapitulation, the ROM is given by Equations 29 through 31, with the only difference that flow parameters D^0 and τ_{mix} are now properties of a turbulent flow. As the ROM captures reaction-dependent effects explicitly, D^0 and τ_{mix} can remain agnostic to the presence of a reacting system, therefore nonreactive flow measurements provide the values needed. Specifically, [8] explicates the process of finding these values for nonreactive turbulent flows using the macroscopic forcing method (MFM). In particular, Ref. [19] used MFM to measure the true nonlocal form of the macroscopic eddy diffusivity, and additionally found values for D^0 in the purely local and isotropic limit applicable for this work.

In this way, the effects of changing flow topology, i.e., from laminar parallel flow to 3D turbulent flow, is implicitly captured via changes in D^0. Specifically, revisiting Equation 4, we see that in the laminar problem, $D^0 \sim u_{\text{rms}}^2 L_2^2/D_m$. In this case, the D_m in the denominator represents the effects of molecular mixing in the spanwise direction as can be tracked in the derivation process presented in

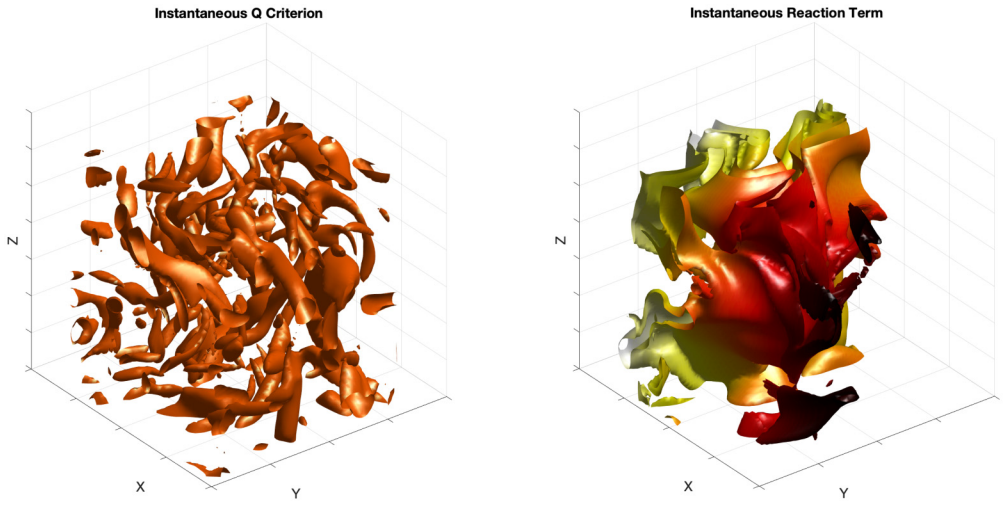

FIG. 5. Instantaneous visualization of a binary reaction system subject to homogeneous, isotropic turbulence at the $\mathrm{Re}_\lambda = 26$ case (a) An isosurface of the instantaneous Q criterion that indicates eddy cores (b) An isosurface of the instantaneous reaction term, AC_1C_2, at 10% of the maximum reaction term, colored by axial coordinate. In both figures, axes are equally scaled.

Sec. II. In the turbulent case, the same concept holds, except that the spanwise mixing is dominated by D^0 itself. This would turn the scaling relation of Equation (4) into $D^0 \sim u_{\mathrm{rms}}^2 L_2^2/D^0$, where L_2 must be replaced by the large eddy size. This eddy size scales as $L_{\mathrm{eddy}} \sim u_{\mathrm{rms}}^3/\epsilon$, where ϵ is the turbulent kinetic energy dissipation rate. This leads to the scaling of $D^0 \sim u_{\mathrm{rms}} L_{\mathrm{eddy}}$ which is the expected scaling and is already captured by the measured D^0 from nonreactive cases.

A. The turbulent setup

Now we replace the steady, parallel flow examined in the previous section with 3D homogeneous isotropic turbulence (HIT) in an elongated domain to generalize the model problem. The Navier-Stokes solver code of Ref. [20] in an incompressible mode was adapted for this work to simulate HIT in a 3D domain of size $(2\pi)^3$. The resulting flow field was periodically extended in the x direction to generate a computational domain for scalar transport with dimensions $20\pi \times 2\pi \times 2\pi$. The scalar transport equations are solved with boundary conditions identical to the 2D binary reaction problem. This provides a realistic reaction zone in the middle of the domain, far from the boundaries, as seen in Fig. 5.

The velocity fields were solved on uniformly spaced structured meshes and to sustain turbulence, the incompressible Navier-Stokes equations are solved with a forcing of Bu_i added to the right-hand side of the momentum equations. B is a turbulence forcing parameter described in Ref. [21]. The solver was run to statistical convergence for $O(500-2000)$ eddy turnover times after discarding initial transients, as prescribed by Ref. [19] and we examine values of $\mathrm{Re}_\lambda = 26$ and $\mathrm{Re}_\lambda = 40$. Following that work, the turbulent forcing parameter is $B = 0.2792$ for both Reynolds numbers. For $\mathrm{Re}_\lambda = 26$, each box is a meshed with 64^3 points and the kinematic viscosity set to $\nu = 0.0263$. For $\mathrm{Re}_\lambda = 40$, each box is meshed with 128^3 points with $\nu = 0.0111$. Five cases, with summary parameters given in Table I, were studied. Estimates of the turbulent statistical quantities, specifically ϵ and u_{rms}, in the table are adapted from [19]. The molecular diffusivity for both scalars is equal to the kinematic viscosity, so the relevant Schmidt number is unity.

This setup allows adoption of the values for nonreactive eddy diffusivity calculated in Ref. [19]. In particular, while the kinematic viscosity, molecular diffusivity, box size, and reaction coefficient

TABLE I. Summary parameters for the turbulent cases considered.

Case	1	2	3	4	5
Da	104	52	26	138	276
Pe	37	37	37	72	72
Re_λ	26	26	26	40	40
u_{rms}	0.97	0.97	0.97	0.905	0.905
ϵ	0.780	0.780	0.780	0.687	0.687

are inputs, all other measured quantities are computed by post-processing the data. For Case 1, for example, Ref. [19] reported that $D^0 = 0.86u_{\mathrm{rms}}^4/\epsilon = 0.976$ and $\tau_{\mathrm{mix}} = 0.86u_{\mathrm{rms}}^2/\epsilon = 1.04$, where $\epsilon = 0.78$ is the dissipation rate of turbulent kinetic energy and $u_{\mathrm{rms}} = 0.97$ is the single-component root-mean-squared velocity.

For scalar transport for Case 1, for example, we consider molecular diffusivity $D_m = 0.0263$, matching ν, $C_{\mathrm{ref}} = 1$ and a reaction rate $A = 100$. This leads to $Pe \equiv D^0/D_m = 37$ and $Da \equiv A\tau_{\mathrm{mix}}C_{\mathrm{ref}} = 104$. The values are similarly calculated for the other cases using the values from Table I.

Figure 5 shows imagery captured near the middle of the computational domain for Case 1 and Fig. 5(a) shows vigorous turbulent structures that mix the flow and the scalar fields. In response, reaction fronts are not planar; instead, one can observe highly stretched and distorted structures. Similar to the laminar problem, however, the ensemble-averaged fields will be smooth and one-dimensional.

B. *A priori* analysis

In Fig. 6, the closure terms for the ensemble-averaged binary reaction problem for Case 1 are examined in the defined turbulent context by performing *a priori* analysis, wherein we plug in DNS-derived mean quantities into the closure expressions. Similar to the laminar binary reaction problem, the full ROM recovers from the errors in capturing the true transport closures that are incurred by the linear reaction model of Equation 22. For these specific closure terms, the standard gradient diffusion model appears to match the DNS data more closely than the ROM. Neither gradient diffusion nor the linear reaction model offer closure to the reaction term, which the ROM does.

In Sec. IV, we will discuss an explanation regarding observed accuracy of gradient diffusion model for the transport closure despite its ignorance of reaction effects. Nevertheless, an overall assessment that considers both reaction and transport closures reveals the advantage of the ROM, as the gradient diffusion transport closure model offers no answers to the equally vital reaction closure question. While there exists a significant quantitative gap in predictions of the reaction closure term between ROM and DNS, this leading order ROM correction consistently captures the magnitude and shape of the reaction closure, without any tuning of the coefficients. This misprediction by roughly half in the scalar source term has implications, as it likely depresses the predicted value of the scalar fields in the flame zone, as the positivity of the term acts as a net source.

These conclusions are the same for each of the other cases considered, but only Case 1 is visually shown, as *a priori* results are just used qualitatively to build confidence in the advantages of the proposed ROM. Quantifying this advantage can be accomplished by performing *a posteriori* analysis and comparing 1D model predictions against DNS data.

C. *A posteriori* analysis

In this section, we solve Equation 2 directly by invoking some of the closure models heretofore presented. We consider the two best performing models from the *a priori* results and omit the Linear

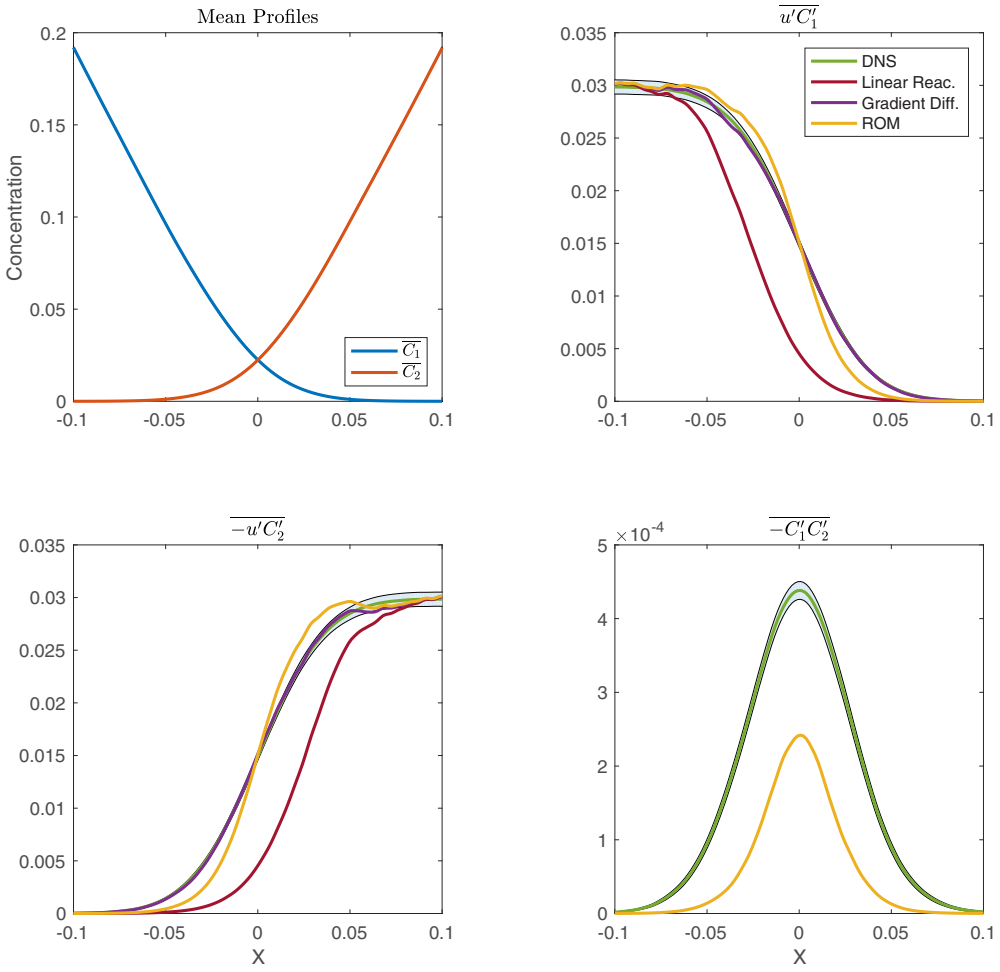

FIG. 6. Predictions of closures for the binary reaction problem subject to a turbulent flow for *a priori* analysis Case 1. $X = x/L_1$ and DNS results are presented with 95% confidence intervals accounting for statistical fluctuations.

Reaction model. The problem setup and parameters used in this section are identical to those for the *a priori* analysis. The primary exception is that for the RANS equation, instead of Dirichlet boundary conditions for the scalars, Neumann boundary conditions with slopes matching the DNS profiles are used. This is done because the DNS develops axial boundary layers near the Dirichlet conditions due to local outflow advection. For the DNS, we have ensured these artificial effects do not pollute the reaction zone results by ensuring the boundaries are far from the reaction zone. These boundary layers are absent in the RANS case as the mean velocity is zero. Appropriate matching of RANS solutions to the DNS ones should consider concentration profiles outside of these artificial boundary layers. We have done so by matching the slopes of the RANS concentration profiles to those of the DNS outside of the boundary layers, but far from the reaction zones.

In Table II, the maximum error in C_1 is tabulated for both models, and it shows that the ROM incurs less error. For illustration, in Fig. 7(a), we compare the predicted mean profiles for Case 1 of C_1 and C_2 to the results derived from the DNS described in the previous section. In Table II, we can demonstrate that the ROM outperforms the standard gradient diffusion model and the error metric is roughly halved.

TABLE II. The maximum absolute value of error in C_1 for the gradient diffusion (GD) and reduced order model (ROM) far from the boundaries, $|X| = |x/L_1| < 0.3$, as compared to the turbulent DNS results for all cases.

Case	1	2	3	4	5
Da	104	52	26	138	276
Pe	37	37	37	72	72
GD Max. Error	1.097×10^{-2}	9.195×10^{-3}	8.007×10^{-3}	1.035×10^{-2}	1.221×10^{-2}
ROM Max. Error	4.590×10^{-3}	3.714×10^{-3}	3.131×10^{-3}	4.811×10^{-3}	5.885×10^{-3}

Next, we examine whether the additional closure terms contribute equally to the final calculated mean quantities. To demonstrate the relative importance of each of the closure terms, Fig. 7(b) shows the effects of toggling each of the closure terms on the overall accuracy of scalar concentration predictions for Case 1. The main feature seen in this plot is that the effects of the two individual closures do not linearly add to the full ROM prediction, and there is still a gap between the ROM and the DNS results. The implications of this misprediction based on the local model form will be addressed in the next section.

In the Appendix, *a posteriori* results for the other cases show that the discrepancy between the DNS results and the ROM does appear consistently. In particular, the role of the reaction closure is a net source for each of the two scalars, so the underprediction of the DNS values shown in the sample *a priori* results of that term continues in each of the flow setups considered.

IV. DISCUSSION AND CONCLUSIONS

In this work, we have introduced a framework to extend the analysis of the dispersion of a single passive tracer to analysis of system of species undergoing binary reactions. The resulting model form derived herein introduces closures to both advective flux and reaction terms with nonlinear interactions between the mean state of all species, even though the primary set of equations being solved undergo a linearization procedure. The proposed framework also captures the nonreactive and linear reaction limits as special cases of the binary reaction problem. In contrast to Ref. [4], the

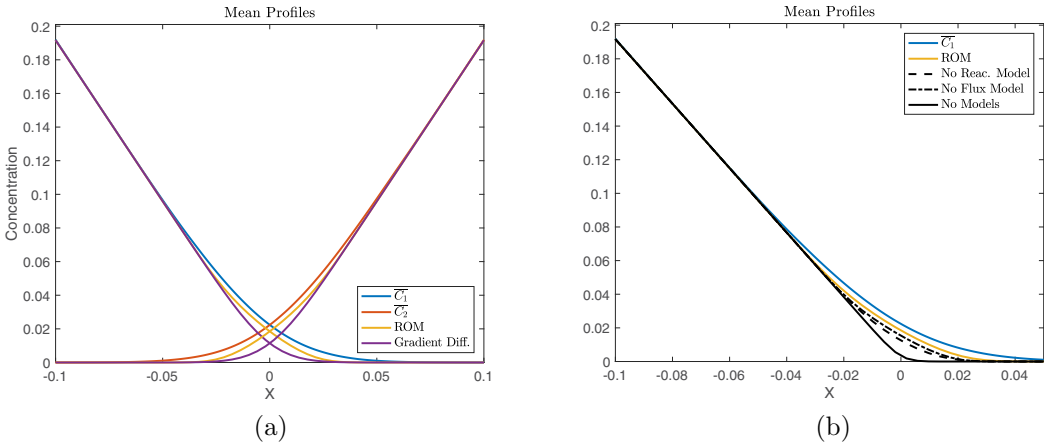

FIG. 7. Results of *a posteriori* analysis for Case 1, with DNS quantities indicated with overbars, $X = x/L_1$. (a) A comparison of the predicted mean scalar profiles in the reaction zone for the ROM and the gradient diffusion models (b) A comparison of the predicted mean scalar profile for C_1 with different aspects of the ROM active.

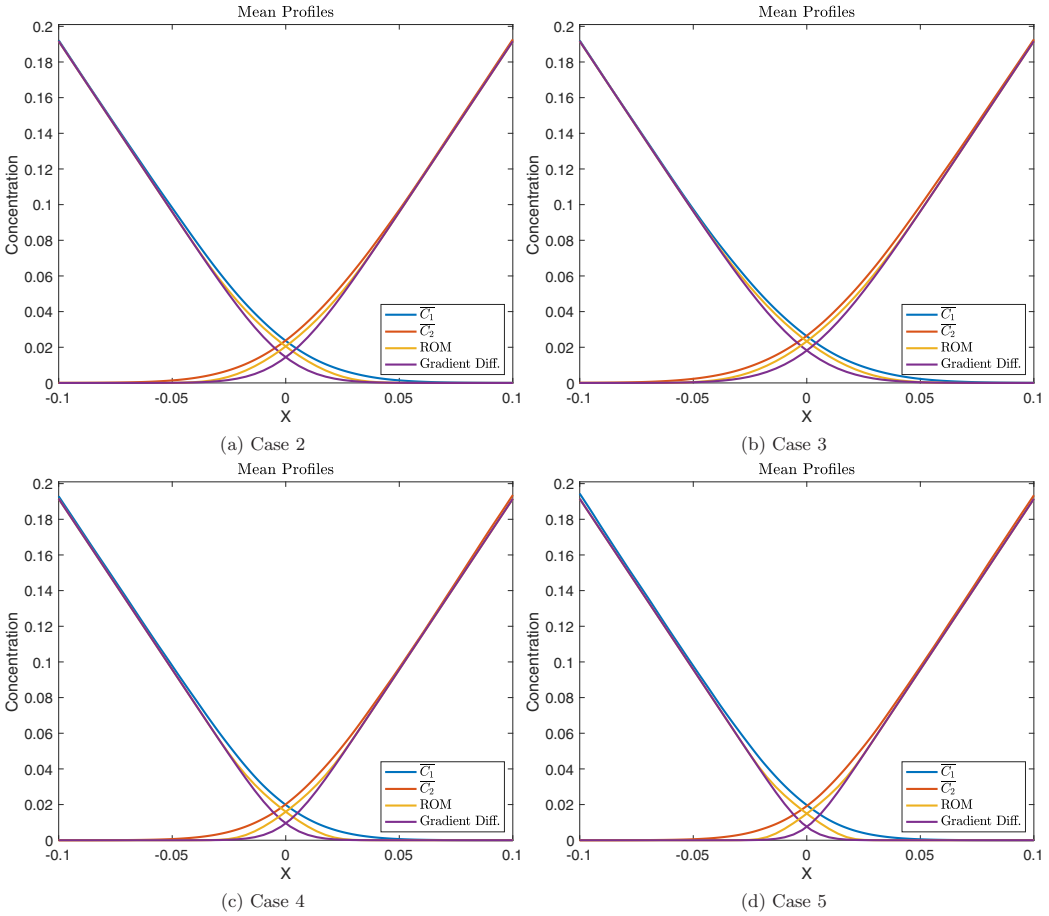

(a) Case 2 (b) Case 3

(c) Case 4 (d) Case 5

FIG. 8. Results of *a posteriori* analysis for Cases 2-5, with DNS quantities indicated with overbars, $X = x/L_1$. A comparison of the predicted mean scalar profiles in the reaction zone is given for the ROM and the gradient diffusion models for each case, as labeled. (a) Case 2(b), Case 3(c), Case 4(d), and Case 5.

derived model leads to a positive-eigenvalue diffusion operator across all Damköhler numbers, so numerical applicability is maintained when the introduced ROM is used in a one-dimensional scalar equation solver.

By considering a prototype laminar and five turbulent test cases, we showed that the standard gradient diffusion and linear reaction model do not suitably capture the behavior of mean scalar fields across all problems. The presently considered ROM, however, can address all these different regimes consistently. Perhaps the most novel aspect of this work is the direct translation of the obtained model form between the laminar prototype problem and the test problem involving turbulent flows. Most critically, no tuning of parameters was used in this analysis, as methods like MFM permit the measurement of D^0 directly for turbulent flows. However, it is unclear whether omitting a constant prefactor in $\tau_{\text{mix}} = D^0/u_{\text{rms}}^2$ is appropriate for turbulent settings. In the laminar case, this definition with no need for an additional prefactor was derived analytically. In the turbulent case, we simply adopted the laminar definition without retuning its prefactor that could otherwise account for the change in flow topology.

An interesting feature of the developed ROM is that advective fluxes of any one reactant depend on mean gradients of other species involved in the reaction. This leads to an effective diffusivity matrix that shows cross-diffusion coefficients. In this sense, our results are consistent with the recent

work of Ref. [22] in which a 2D system undergoing a slightly different reaction mechanism was considered. However, the additional advantage of the recent ROM is that it consistently models all multiphysics effects by offering closure expressions to both reaction terms as well as transport terms. Furthermore, the present ROM provides analytic model forms that capture explicitly the influence of reaction constants on each closure operator. To this end, the only other inputs needed are the nonreactive eddy diffusivities and the mixing time scale to form the appropriate Damköhler numbers.

It should be noted that this analysis is not identical to reacting flow formulations that consider just a mixture fraction or related quantity, as covered canonically in Ref. [23] or in literature such as Ref. [24], as the primary scalar. The mixture fraction maps both concentration fields in a binary system to a single scalar that is conserved in space. This is in contrast to the partial differential equations considered here.

While the developed ROM is not directly implementable in a complex combustion problem, we hope this framework introduces insights into the model form one could expect for the general class of reaction–advection–diffusion problems. In Supplemental Material given in Ref. [18], we demonstrate that including a higher order correction that captures nonlinear effects does not make a model created in a laminar context more able to capture turbulent effects. We therefore conclude that the leading order model is the extent of the correspondence between the laminar and turbulent contexts.

The remaining error between DNS results and ROM predictions in the *a posteriori* analysis can be attributed to the lack of consideration of nonlocal effects in the derivation of our model form. In the high $Da = A_L \tau_{\text{mix}}$ linear reaction case, the effective reaction length scale, l as in Equation 32, is inevitably less than the flow mixing length, L, given by the large eddy length. This can be assessed by a series of inequalities, as show below, noting that D_{eff} is reduced in the presence of reaction.

$$l \sim \sqrt{\frac{D_{\text{eff}}}{A_L}} < \sqrt{\frac{D^0}{A_L}} < \sqrt{D^0 \tau_{\text{mix}}} \sim L. \tag{32}$$

As a result, in the turbulent case, the energy-containing eddies are far larger than the chemically active zone. This nonlocal mixing implies that the closure terms, such as $\overline{u'c'}$, should also be nonlocal. Finding the kernel for this nonlocal model form will require techniques such as MFM to analyze the range of this dependence. So, future work may be focused on capturing nonlocality, as in Refs. [19,25], which should account for the discrepancy of the ROM values and the DNS measurements.

Another promising avenue of further inquiry is applying the proposed ROM to a large-eddy simulation context as a subgrid-scale model, where mean space variables are replaced with filtered variables and quantities like u_{rms} are evaluated at the grid scale.

ACKNOWLEDGMENTS

O.S. was supported by the National Science Foundation Graduate Research Fellowship Program under Grant No. 1656518 and the Stanford Graduate Fellowships in Science and Engineering. This work was supported by the Office of Naval Research under Grant No. N00014-20-1-2718. Computational resources were provided by NSF Extreme Science and Engineering Discovery Environment resources under Grant No. CTS190057 and the Department of Energy, National Nuclear Security Administration under Award No. DE-NA0003968.

APPENDIX: FURTHER *A POSTERIORI* RESULTS

In this section, Fig. 8 illustrates *a posteriori* results for Cases 2–5, as was done in Fig. 7 for Case 1. The basic trends highlighted for Case 1 in the main text continue in each of the considered cases, regardless of the change of macroscopic parameters as captured in Table II. This implies that the

local ROM does not capture some multiphysics correctly, which could be remedied by the use of a nonlocal model form.

[1] J. H. Seinfeld and S. N. Pandis, *Atmospheric Chemistry and Physics : From Air Pollution to Climate Change*, third edition. (Wiley, Hoboken, New Jersey, 2016)

[2] N. Peters, *Turbulent Combustion*, Cambridge Monographs on Mechanics (Cambridge University Press, Cambridge, 2000).

[3] M. Rosales and J. L. Nava, Simulations of turbulent flow, mass transport, and tertiary current distribution on the cathode of a rotating cylinder electrode reactor in continuous operation mode during silver deposition, J. Electrochem. Soc. **164**, E3345 (2017).

[4] I. Battiato and D. Tartakovsky, Applicability regimes for macroscopic models of reactive transport in porous media, J. Contam. Hydrol. **120-121**, 18 (2011).

[5] H. Pitsch, Large-eddy simulation of turbulent combustion, Annu. Rev. Fluid Mech. **38**, 453 (2006),.

[6] J. D. Avrin, Incompressible reacting flows, Trans. Amer. Math. Soc. **349**, 3875 (1997).

[7] R. H. Kraichnan, Eddy viscosity and diffusivity: exact formulas and approximations, Complex Syst. **1**, 805 (1987).

[8] A. Mani and D. Park, Macroscopic forcing method: A tool for turbulence modeling and analysis of closures, Phys. Rev. Fluids **6**, 054607 (2021).

[9] G. I. Taylor, Dispersion of soluble matter in solvent flowing slowly through a tube, Proc. R. Soc. London A **219**, 186 (1953).

[10] G. I. Taylor, The dispersion of matter in turbulent flow through a pipe, Proc. R. Soc. London A **223**, 446 (1954).

[11] R. Aris, On the dispersion of a solute in a fluid flowing through a tube, Proc. R. Soc. London A **235**, 67 (1956).

[12] M. J. Lighthill, Initial development of diffusion in Poiseuille flow, IMA J. Appl. Math. **2**, 97 (1966).

[13] M. Shapiro and H. Brenner, Taylor dispersion of chemically reactive species: Irreversible first-order reactions in bulk and on boundaries, Chem. Eng. Sci. **41**, 1417 (1986).

[14] S. Corrsin, The reactant concentration spectrum in turbulent mixing with a first-order reaction, J. Fluid Mech. **11**, 407 (1961).

[15] T. Elperin, N. Kleeorin, M. Liberman, and I. Rogachevskii, Turbulent diffusion of chemically reacting gaseous admixtures, Phys. Rev. E **90**, 053001 (2014).

[16] T. Elperin, N. Kleeorin, M. Liberman, A. N. Lipatnikov, I. Rogachevskii, and R. Yu, Turbulent diffusion of chemically reacting flows: Theory and numerical simulations, Phys. Rev. E **96**, 053111 (2017).

[17] T. Watanabe, Y. Sakai, K. Nagata, and O. Terashima, Turbulent schmidt number and eddy diffusivity change with a chemical reaction, J. Fluid Mech. **754**, 98 (2014).

[18] See Supplemental Material at http://link.aps.org/supplemental/10.1103/PhysRevFluids.7.093201 for an examination of higher-order nonlinear effects.

[19] Y. Shirian and A. Mani, Eddy diffusivity operator in homogeneous isotropic turbulence, Phys. Rev. Fluids **7**, L052601 (2022).

[20] H. Pouransari, M. Mortazavi, and A. Mani, Parallel variable-density particle-laden turbulence simulation, arXiv:1601.05448.

[21] C. Rosales and C. Meneveau, Linear forcing in numerical simulations of isotropic turbulence: Physical space implementations and convergence properties, Phys. Fluids **17**, 095106 (2005).

[22] C. J. Prend, G. R. Flierl, K. M. Smith, and A. K. Kaminski, Parameterizing eddy transport of biogeochemical tracers, Geophys. Res. Lett. **48**, e2021GL094405 (2021).

[23] S. B. Pope, *Turbulent Flows* (Cambridge University Press, Cambridge, 2000).

[24] H. Wang, M. Sun, Y. Yang, and N. Qin, A passive scalar-based method for numerical combustion, Int. J. Hydrogen Energy **40**, 10658 (2015).

[25] J. Liu, H. Williams, and A. Mani, A systematic approach for obtaining and modeling a nonlocal eddy diffusivity, arXiv:2111.03914.